Sensors and Actuators A 188 (2012) 434–441

Contents lists available at SciVerse ScienceDirect

Sensors and Actuators A: Physical

journal homepage: www.elsevier.com/locate/sna

Suspended and highly aligned carbon nanotube thin-film structures using open microfluidic channel template

Dongjin Lee[a,c,1], Zhijiang Ye[a,1], Stephen A. Campbell[b], Tianhong Cui[a,*]

[a] Department of Mechanical Engineering, University of Minnesota, 111 Church St. S.E., Minneapolis, MN 55455, USA
[b] Department of Electrical and Computer Engineering, University of Minnesota, 200 Union St. S.E., Minneapolis, MN 55455, USA
[c] School of Mechanical Engineering, Konkuk University, 120 Neungdong-ro, Gwangjin-gu, Seoul 143-701, Republic of Korea

ARTICLE INFO

Article history:
Received 29 September 2011
Received in revised form 14 June 2012
Accepted 14 June 2012
Available online 23 June 2012

Keywords:
Carbon nanotube
Alignment
Microfluidics
Suspended CNT thin film
NEMS switch

ABSTRACT

We demonstrate microfabrication and characterization of suspended carbon nanotube (CNT) thin-film structures possessing a high degree of alignment. The alignment of CNT was achieved by the open microfluidic channel template and enhanced by heating the CNT dispersion, which was scalable and processable. The degree of alignment, as characterized by Raman spectroscopy, yielded a high G- to D-band intensity ratio of 22 along the fluid flow direction. The microfluidic alignment scheme was combined with microfabrication techniques for the fabrication of suspended thin-film structures. The sidewall of CNT film pattern, left in fluidic channel removal process, was successfully removed by oxygen plasma etching with a masking layer of photoresist, as shown by scanning electron microscopy and atomic force microscopy. The resistivity of the aligned CNT film was found to be $2.2 \times 10^{-3}\ \Omega$ cm, smaller than that of films aligned by other techniques. The aligned CNT film was released by etching a sacrificial layer. Mechanical characterization showed a nominal Young's modulus of 635 GPa and yield strength of 2.4 GPa on the assumption of a fixed–fixed Euler beam. The reliable, scalable and processable fabrication process, the resulting high conductivity and excellent mechanical properties may enable aligned CNT films to be a potent candidate for electromechanical device applications.

1. Introduction

Since the discovery of carbon nanotubes (CNTs), they have garnered much attention in both academic and industrial sectors for novel device applications such as transistors [1,2], light emitting diodes [3], sensors [4–7] and electromechanical switches [8]. CNT-based electromechanical switches made as suspended bridges across two anchoring electrodes revealed a high switching speed and low actuation voltage on the range of 1–10 V [8–10]. Most CNT-based electromechanical switches were implemented as individual one-dimensional (1D) nanostructures through either in situ growth or post-growth assembly. In situ growth of individual CNTs on a patterned substrate requires a high synthesis temperature (~400 °C), which might be a hurdle for integrating with CMOS or using a flexible polymer substrate. Furthermore, manipulating individual CNTs as a post-growth assembly for the integration into a host device structure is extremely challenging and unlikely to be manufacturable. Instead of using individual CNTs, therefore, we reported the reliable fabrication of the suspended CNT nanocomposite thin-film structure through the combination of lithographic technique and layer-by-layer nano-self-assembly [11]. The electrical and mechanical properties of randomly networked CNT composite thin-film were elucidated upon release of the film.

In addition to the development of a reliable fabrication scheme, the alignment of a 1D nanomaterial has been of great interest as a functional nanostructure for enhancement of device performance. The alignment of a 1D nanomaterial may adjust the mechanical strength [12], electrical or thermal transport phenomenon [13], and tune the anisotropy of host materials [14]. A futuristic application of CNTs in electromechanical switches requires a good electrical conductivity with excellent mechanical properties, which is targeted for high speed device application. For this reason, aligned CNT films have been spotlighted as a functional nanostructure suitable for nanoelectronics due to the relieved fabrication challenge [5] while preserving the ballistic properties [2]. Indeed, the selective placement and controllable orientation of CNTs along with a large-area capability are essential, being compatible with current silicon-based fabrication techniques for scale-up production. In addition, the post-growth assembly and alignment are of great importance when considering CNTs as an off-the-shelf raw building component. Aligned CNT thin-films made by dielectrophoresis was reported to have a better mechanical properties [15] and electrical device performance [16] than a film with randomly distributed

* Corresponding author. Tel.: +1 612 626 1636; fax: +1 612 625 6069.
E-mail address: tcui@me.umn.edu (T. Cui).
[1] These authors contributed equally to this work.

0924-4247/$ – see front matter © 2012 Elsevier B.V. All rights reserved.
http://dx.doi.org/10.1016/j.sna.2012.06.013

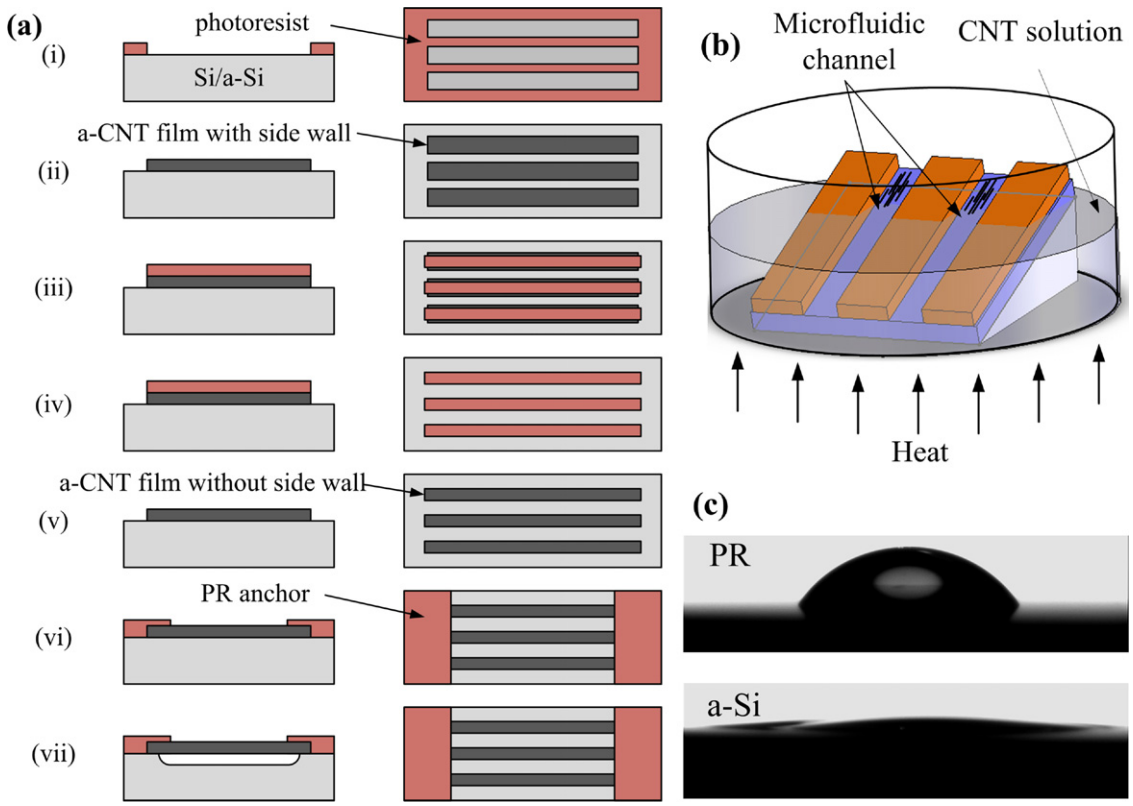

Fig. 1. Suspended and aligned carbon nanotube thin-film structure using open microfluidic channel template: (a) beam fabrication flowchart ((i) photoresist microfluidic channel fabrication, (ii) CNT alignment and lift-off, (iii) to (v) sidewall removal process with oxygen plasma etching, (vi) photoresist anchor fabrication, (vii) beam release by sacrificial layer etching), (b) schematic of thermally enhanced microfluidic template guided aligning scheme, and (c) contact angle measurement before the alignment revealing hydrophobic photoresist channel (top) and superhydrophilic a-Si surface (bottom) that are suitable for CNT alignment. In (a), left column shows cross section view whilst right depicts top view. CNT solution evaporated at 80 °C so that 3-phase line moves down leaving aligned CNTs along fluidic channels.

CNTs. However, the dielectrophoretic approach lacks the capability of both selective placement and alignment over a large area, and requires an electrode pattern for the application of an electric field [17]. The capillary force induced alignment of selectively grown CNTs [18] was demonstrated for the fabrication of 3D MEMS devices [19]. Here we demonstrate that the microfluidic approach was scalable, highly reproducible and processable compared to other techniques, achieving a high degree of alignment along the fluid direction [20].

In this study, therefore, aligned CNT films are fabricated by means of a microfluidic template alignment scheme [20] and suspended fully using lithographic techniques for the application of MEMS switch [11]. Due to different micropatterning techniques, the fabrication process was modified to address the issues of sidewall and etching of sacrificial layer. The fabrication procedure is described with emphasis on the successful release of the aligned CNT films. The aligned CNT film is characterized electrically and mechanically in the form of a 2D film on the substrate and a 3D film suspended between two anchors, respectively, revealing a film resistivity of $2.2 \times 10^{-3}\ \Omega$ cm and a Young's modulus of 635 GPa. Aligned CNT films, as stiff and conductive nanostructures, are a potential candidate for electromechanical devices such as high speed radio frequency (RF) switches.

2. Experiment

The fabrication of the suspended aligned CNT thin-film beam involved a combination of microfluidic alignment [20] and CNT device fabrication techniques [11]. The fabrication flowchart is shown in Fig. 1(a). Starting with well cleaned silicon (Si) wafer, amorphous silicon (a-Si) was deposited using plasma enhanced chemical vapor deposition (PECVD) at 150 °C. It served as a sacrificial layer for beam release as well as dielectric layer for electrical characterization of the aligned SWCNT film. The thickness was around 1 μm in order to accommodate the deflection when the suspended CNT thin-film beams were tested using the nanoindenter afterward. Microfluidic templates were fabricated by patterning a positive photoresist (PR, Shipley S1813) using photolithography (step i). The fabricated open channel width and height were 4 and 1.3 μm, respectively. After oxygen (O_2) plasma treatment of the template at a power of 100 W and an O_2 flow rate of 100 sccm for 1 min, the wafer was soaked in a developer solution for 5 s to obtain the surface wetting properties suitable for CNT alignment. This surface treatment scheme yielded hydrophobic channel sidewalls and a hydrophilic channel bottom, which was crucial in alignment of CNTs. Subsequently, the fluidic channel was dipped into SWCNT dispersion (PureTubes^{TM}, Nanointergris Inc., 0.25 wt%, diameter of 1.2–1.7 nm and length of 0.3–4 μm) with a tilt angle of about 20° and the bottom surface of CNTs solution container was placed on a hotplate at 80 °C to expedite the evaporation as shown in Fig. 1(b). Following lift-off of the PR channel in acetone (step ii), a 2nd lithography step was used to remove the sidewall (step iii). The etch was done for 3 min in a 150 W O_2 plasma with an O_2 flow rate of 100 sccm (step iv). After PR strip (step v), the mechanical anchor was fabricated for suspended beams with lithography (step vi). The micropattern of PR on both ends of aligned SWCNT film played

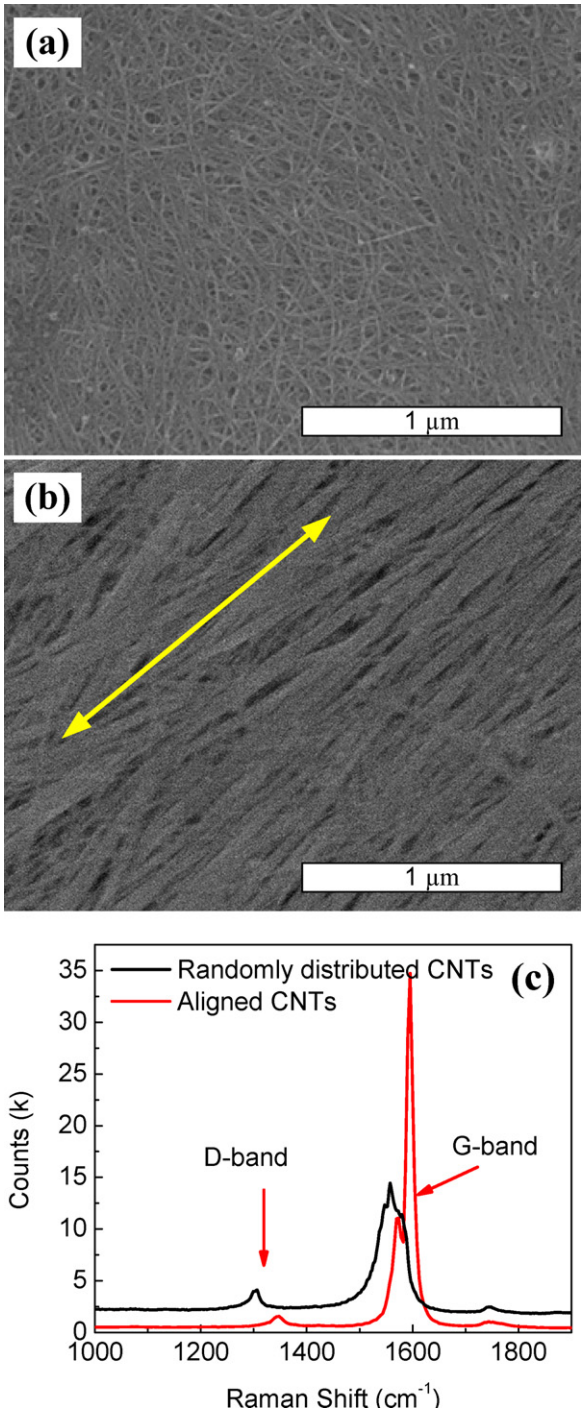

Fig. 2. Comparison of randomly distributed and aligned CNTs on the Si/a-Si substrate formed at 80 °C with 0.25 wt% CNT dispersion concentration: SEM images of randomly networked (a) and aligned CNTs (b), and representative Raman spectra (c) taken with the laser polarized parallel to microfluidic flow direction. G/D band ratios were found as 3.5 and 22 for randomly distributed and aligned CNTs, respectively, which is strong indication of the directional alignment. The arrow indicates the direction of alignment.

a role of the mechanical anchor. PR was used as the anchor for simple mechanical test, however a metal anchor was substituted for the electrical characterization of aligned CNT film. In this case, chromium/gold was sputtered and patterned as both anchors and electrodes. Finally, the a-Si was etched using a 300 W SF_6 plasma at a flow rate of 200 sccm producing a pressure of 300 mTorr (step vii).

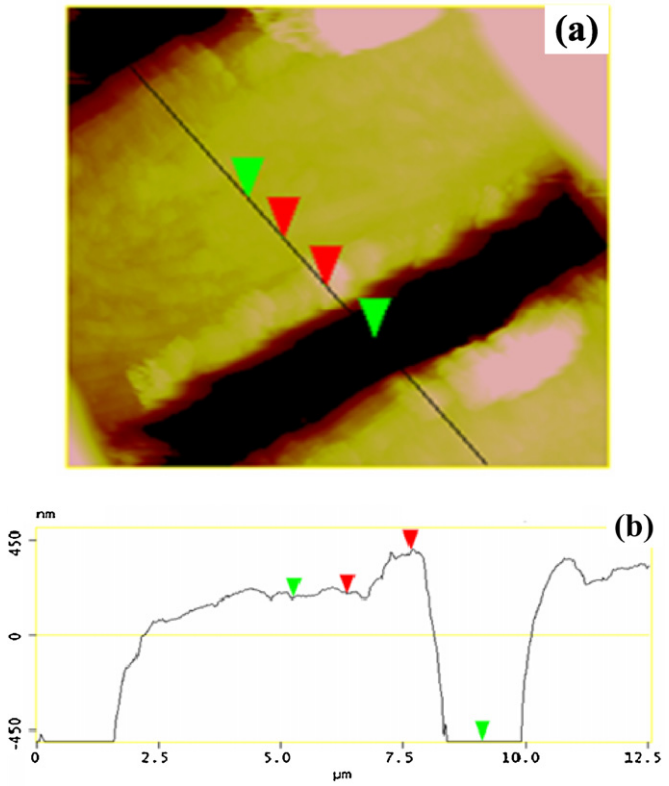

Fig. 3. Suspended CNT beam structure without side-wall removal process: (a) AFM topology image in tapping mode and (b) surface profile along the line indicated in (a). The beam was supposed to be 5 μm wide possessing 5 μm spacing between beams. The beam tended to be wider whereas spacing becomes narrower presumably due to the straightening of the side-wall.

3. Results and discussion

For CNTs to be aligned in the microfluidic template, the surface treatment is one of key parameters. We discovered a lithographic method to control surface wetting properties suitable for microfluidic template guided CNT alignment. Generally, photolithography results in more hydrophobic channel walls than the bottom. After an O_2 plasma treatment at 100 W and an O_2 flow rate of 100 sccm for 1 min, a superhydrophilic surface was obtained on the photoresist fluidic channel wall, while the channel bottom is slightly hydrophobic. Dipping of microfluidic template into developer solution again for 5–10 s altered the surface wetting property, resulting in a hydrophobic channel wall (water contact angle of 53°) and superhydrophilic channel bottom as shown in Fig. 1(c). This surface wetting property facilitated the alignment of CNT. We could not observe well-aligned CNT film using microfluidic channel templates after photolithographic patterning or O_2 plasma treatment. Re-develop of PR template was essential for the CNT alignment in this study.

Raman spectroscopy (Alpha 300R, WITec) was used to compare the aligned CNT film with the randomly networked CNT film that had been fabricated by drop drying on the fluidic channel without tilting the substrate followed by lift-off in acetone. Raman spectroscopy has been widely used for characterizing the purity and ordering of CNTs [21,22]. In the Raman spectrum the G-band is induced by the ordered graphitic structure while the D-band is caused by disorder [21]. The G-band to D-band intensity ratio (G/D band ratio) is typically used to quantify the degree of alignment [20,23] provided that individual CNTs have the same quality. SEM images of randomly distributed and aligned CNT by microfluidic

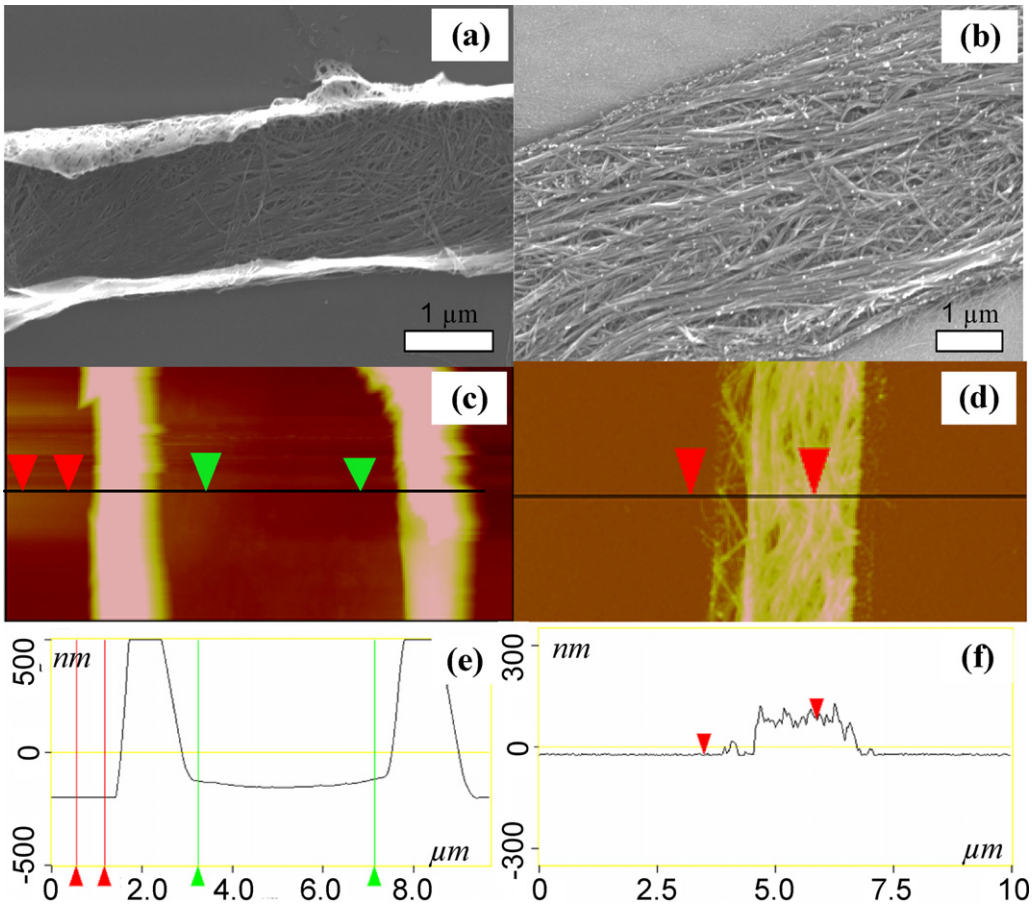

Fig. 4. The effect of oxygen plasma (O_2) etching for the removal of sidewall: SEM images of aligned CNT film (a) before and (b) after side-wall removal, AFM topography (c) before and (d) after side-wall removal, and surface profile across the beam (e) before and (f) after removal of sidewall. The side-wall was removed completely after O_2 plasma treatment.

template are shown in Fig. 2(a) and (b), respectively. The alignment of the CNTs along the direction of the fluidic channel, expressed by the arrow in the figure, is clearly observed in (b), whereas no evidence of alignment is revealed in (a). The Raman spectra were collected with the laser polarized along the direction of microfluidic channel at the wavelength of 514.5 nm and a power of 5 mW for 5 s. The G/D band ratio was found as 3.5 and 22 for randomly distributed and aligned CNTs, respectively. As CNTs become aligned along a certain direction, the D-band intensity decreases and the G-band intensity increases due to the enhanced graphitic matches among CNTs [20]. We performed both SEM and Raman characterization for the aligned CNTs film fabricated at the evaporation temperature of 20–95 °C with microfluidic channel width of 2–5 μm using 0.25, 0.188 and 0.125 wt% of CNT dispersion [20]. As a result, a higher degree of alignment was observed when higher temperature, narrower microfluidic channel width and lower CNT dispersion were used. Among those, the effect of evaporation temperature was the most important parameter in controlling a degree of alignment.

The removal of side-wall of aligned CNT thin-film was one of key processes that enabled the successful release of aligned CNT film without distortion of the beam dimensions. Unlike an etching process [11], the lift-off process, which is described as step ii in Fig. 1(a), generally leaves tall side fences as shown in Fig. 3. The side-wall was occasionally as high as 1 μm, close to the height of microfluidic PR template depending on the lift-off process. The existence of a sidewall may be problematic for applications of novel CNTs thin-film in functional electromechanical devices. For example, when using the film for forming the beam for transducers, it increases the moment of inertia and spring constant of the beams, eventually causing the increase in pull-in voltage of the electromechanical switch.

We addressed the side-wall issue by using O_2 plasma etching with PR mask. The etching mask was designed such that the width was 1–2 μm smaller than microfluidic channel width. The removal of the fence in the aligned CNT film was verified with SEM and AFM as shown in Fig. 4. The SEM images in Fig. 4(a) and (b) clearly demonstrates the removal of the fence. The surface morphology across the film exhibited the fairly high fence as shown in Fig. 4(c) and (e). It ranges from 0.3 to 1.3 μm depending on the lift-off process. On the other hand, the film after O_2 plasma etching shows no evidence of sidewall as observed in Fig. 4(d) and (f). Although a thin layer of side-wall traces may be found as shown in Fig. 4(d) and (f), it could be completely removed in the release process. Consequently, the significant fence height was removed by O_2 plasma etching as shown in Fig. 4(f).

The fence removal process resulted in a narrowing of the aligned CNT film patterns. The microfluidic channel originally had a 5 μm width and 5 μm spacing. When the fabrication was used without a side-wall removal (steps iii–v), it resulted in atomic force microscopy topology as shown in Fig. 3(a). The tapping mode was to minimize the shear interaction of AFM tip with the side wall of aligned CNT thin-film to avoid dimensional distortion. Nonetheless, the beam width is larger than 5 μm and gap between consecutive beams is smaller than 5 μm as indicated in Fig. 3(b). The beam

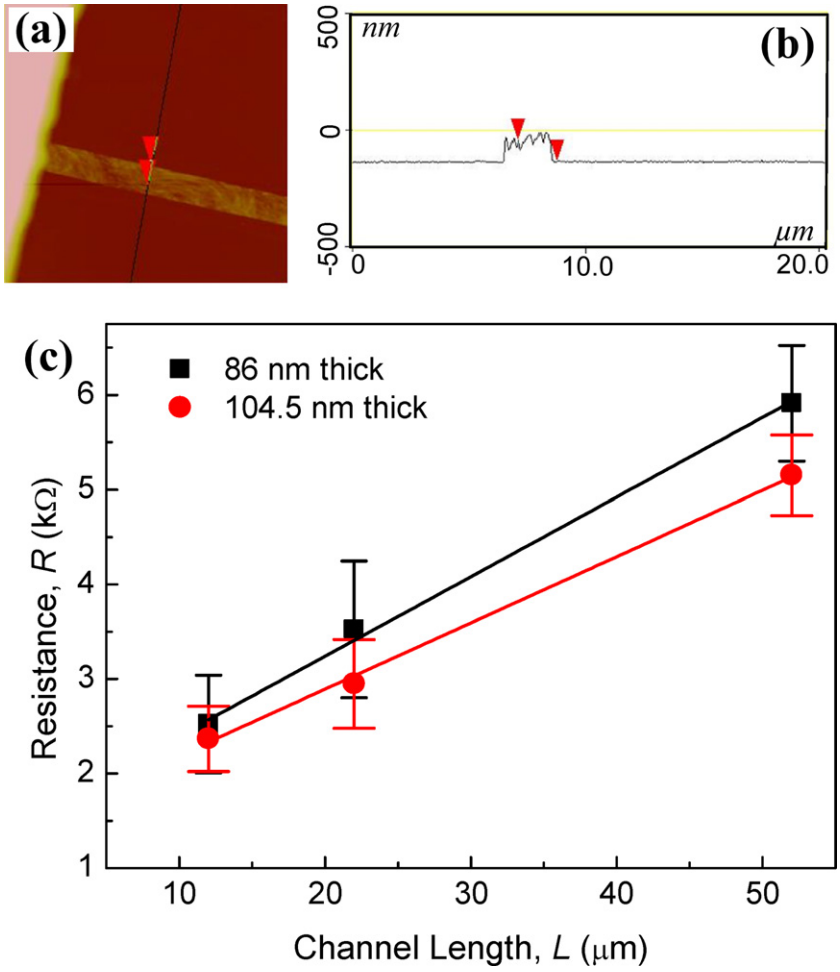

Fig. 5. Electrical characterization of a single 3 μm wide beam on Si/a-Si substrate: (a) exemplary AFM topological image, (b) height profile along the lines indicated in (a) resulting in film thickness of 86 nm, and (c) plot of resistance versus channel length. The fitted line showed the relationship of $R = 84.1L + 1558$ and $R = 70.1L + 1491$, respectively, leading to the film resistivity of $2.2 \times 10^{-3}\ \Omega$ cm. The error bar indicates the standard deviation.

seems to be wider whereas spacing becomes narrower presumably due to the straightening of the side wall.

Instead of a photoresist mechanical anchor, as described as step *vi* in fabrication flowchart, a metallic layer of chromium/gold (Cr/Au) was sputter-deposited onto both anchor and provided an electrical contact to characterize the aligned CNTs film. The thin-film had a 3 μm width and lengths of 12, 22 and 52 μm. AFM was used to measure the thickness of thin-film before the release as shown in Fig. 5(a). The surface profile in Fig. 5(b) along the line indicated in (a) revealed the film thickness of 86 nm. Another film with thickness of 104.5 nm, characterized as in Fig. 4(d) and (f), was also used for electrical characterization. *I–V* measurement was conducted and resistance was extracted on the range of −0.5 to 0.5 V from two-terminal contact devices. The fitted lines in Fig. 5(c) demonstrated a linear relationship of $R = 84.1L + 1558$ ($R^2 = 0.998$) and $R = 70.1L + 1491$ ($R^2 = 0.996$), respectively, for 86 and 104.5 nm thick films. Here, R is the resistance in Ω and L is the channel length in μm. The error bars indicate the standard deviation from 10 different devices. The resistivity and contact resistance were calculated as $2.17 \times 10^{-3}\ \Omega$ cm and 780 Ω for the 86 nm thick film and as $2.21 \times 10^{-3}\ \Omega$ cm and 745 Ω for the 104.5 nm thick film. It is noted that the aligned film yielded the same resistivity. Furthermore, the resistivity is almost 4 times smaller than the aligned film formed by dielectrophoresis [17] presumably due to densely packed and uniformly aligned CNTs. Indeed, microfluidic alignment manufactures dense CNT film possessing a high degree of alignment for the structural application.

The suspended CNT thin-film beam with a high degree of alignment was characterized by SEM to demonstrate the structural sustainability. The film was released entirely over the large area as shown in Fig. 6(a), where the suspended beam array is shown. Furthermore, the alignment of CNTs was maintained after the release process as shown in Fig. 6(b). It is evident that SF_6 plasma did not impair the alignment of CNTs. The suspension of the film manifested itself with the aid of Fig. 6(c) that was focused on the beam edge with the blurred etched a-Si surface as a background. The confocal microscopy was used to confirm the fully suspended beam, resulting in two distinct reflected peaks on the film. It meant that there was the space between the suspended beam and etched surface. Furthermore, the effect of O_2 plasma has been verified to completely remove the side-wall. In addition, PR successfully played a role of the mechanical pads for suspended beam structures as shown in Fig. 6(d). The segregation of CNT film from the PR pad was not observed even after the mechanical characterization with the nanoindenter tip, which will be discussed later. Consequently, microfluidic template guided CNT alignment followed by microfabrication of the suspended beam structure is scalable and processable technique suitable for electromechanical devices.

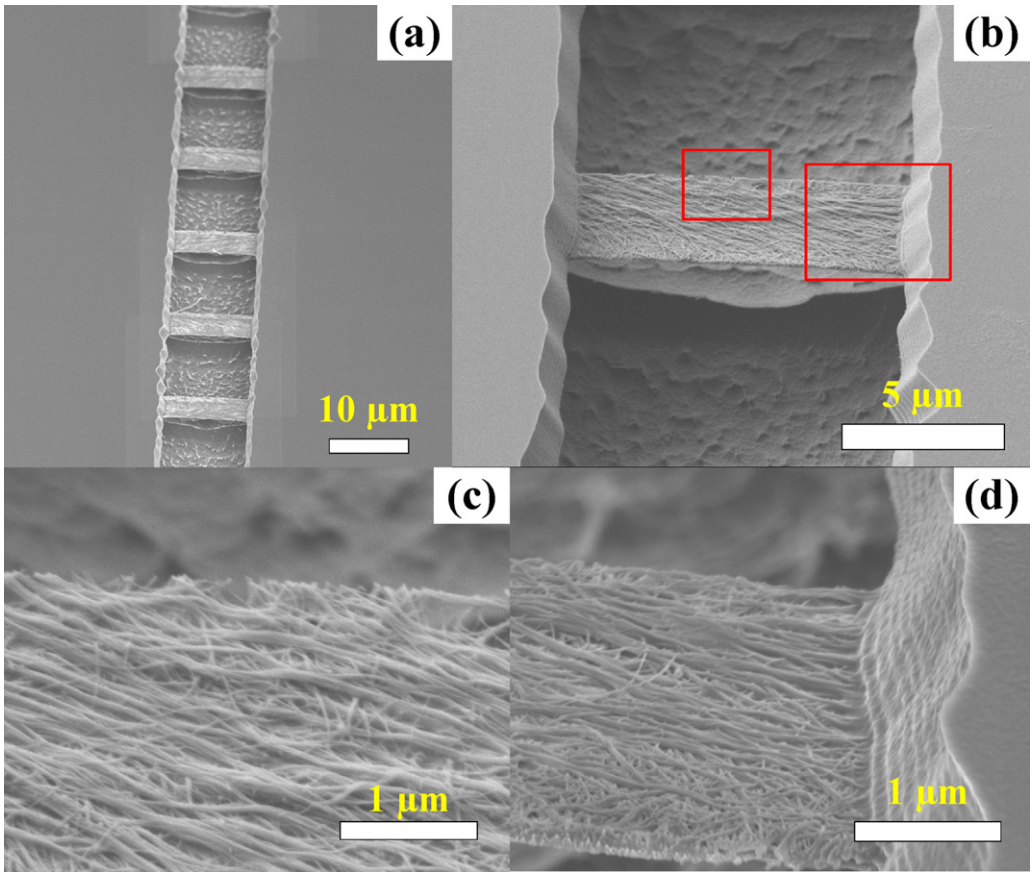

Fig. 6. Scanning electron microscopy image of suspended CNTs beam structures: the images are shown with 60° tilted angle. The alignment of CNTs was maintained after release. (a) Array of suspended beams, (b) a single beam with a high degree of alignment of CNTs, (c) the beam edge that demonstrates clear CNTs and blurred etched surface, and (d) photoresist mechanical anchor pad that depicts a good structural integrity.

The mechanical properties of the suspended beams were characterized with tribonanoindenter (TI 900 Triboindenter, Hysitron) having the Bercovich tip with a tip diameter of 1 μm. This ensures that the indenter does not penetrate into the CNT film so that the indent depth measured in the indentation process is considered the beam deflection. Firstly, the suspended beam sample was placed under the indenter tip that was capable of scanning the sample surface with a force of 2 μN. Then the tip was placed on the center of the beam and started exerting the specified load function. Two kinds of suspended beams with a different thickness were tested and typical load–deflection curves on each sample were demonstrated in Fig. 7(a). The inset shows the load function used, where the load increased linearly with the time from 2.5 to 20 μN and decreased linearly in load-controlled mode. The deflection increased linearly with the load in the elastic region beyond which the load significantly increased to produce the same deflection compared to elastic region. The linear relationship on initial stage of loading was not observed for the aligned CNT film on the substrate as a control. The abrupt increase in load may be attributed to the penetration of the indenter tip into the film presumably upon the yield of the top surface of the beam on which Hertz contact mechanics come into play along with the beam deflection theory. The abrupt increase in load is different behavior from gold nanowire [24], where the load to produce the same amount of deflection decreased due to the ductility of gold. Particularly, it is noted that the linear relation between load and deflection spans over a couple of hundreds of nanometer in deflection, a few times of beam thickness. The yield point at fixed-fixed beam configuration has been extracted from the point where the experimental values start to deviate from the theoretical calculation [24]. The spring constants (k) and the force on yielding (F_y) were extracted on the elastic region and yield points, respectively, as shown in Fig. 7(b). The suspended beam with the mechanical anchor at both ends can be modeled as fixed-fixed beam based on a good structural integrity observed in Fig. 6. Young's modulus (E) and yield strength (σ) of the structural beam material are extracted from Euler beam theory as follows:

$$E = \frac{L^3 k}{16\, w t^3}$$

$$\sigma = \frac{3 F_y L}{4 w t^2}$$

where w, t, and L are the width, thickness, and length of the beam, respectively. Two kinds of samples with 92 and 115 nm thickness measured by AFM were tested and the data were summarized as shown in Table 1. Consequently, Young's modulus of 635 GPa and yield strength of 2.4 GPa were found. A high Young's modulus with a high elastic deflection makes this structural material a potential candidate for electromechanical switch application.

Table 1
Sample description and mechanical properties found in nanoindentation test.

Sample	Thickness (nm)	Average		E (GPa)	σ (GPa)
		k (N/m)	F_y (μN)		
Group I	92	18.6 ± 1.7	7.1 ± 1.8	626 ± 55	2.3 ± 0.5
Group II	115	37.3 ± 1.9	12.3 ± 2.6	644 ± 35	2.5 ± 0.5

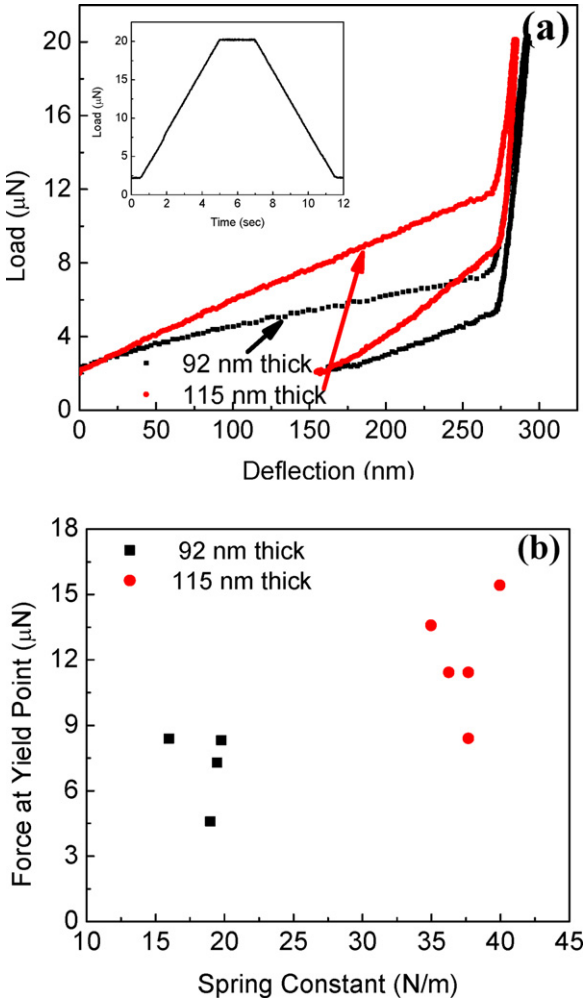

Fig. 7. Mechanical characterization of 3 μm wide and 10.8 μm long suspended CNT beams with nanoindentation: Two kinds of thicknesses are tested as shown in Table 1. (a) Typical load–deflection curves (inset: load function applied), (b) extracted force at yielding point versus spring constant found in the linear elastic region from which yield strength (σ) and Young's modulus (E) are extracted as shown in Table 1.

4. Conclusion

In summary, we have utilized thermally enhanced microfluidic template guided alignment scheme in order to fabricate suspended bridges targeted for nanoelectromechanical switch application. The microfluidic alignment is proven to be an effective way of fabricating dense films and realizing a high degree of alignment, which is scalable and processable for the manufacture of the structurally functional CNT nanostructure. The lithography-compatible techniques successfully make the suspended bridge with a high degree of alignment. The resistivity of aligned CNTs film is found as 2.2×10^{-3} Ω cm and the indentation test showed a nominal high Young's modulus of 635 GPa and yield strength of 2.4 GPa. The conductive CNT film has excellent mechanical properties and could be an excellent candidate for electromechanical device applications.

Acknowledgments

This work was supported by the DARPA NEMS Program. We acknowledge the Nanofabrication Center, University of Minnesota, which is supported by NSF through NNIN program. Parts of this work were carried out in the College of Science and Engineering Characterization Facility, University of Minnesota, which was partially supported by NSF.

References

[1] R. Martel, T. Schmidt, H.R. Shea, T. Hertel, P. Avouris, Single- and multi-wall carbon nanotube field-effect transistors, Applied Physics Letters 73 (1998) 2447–2449.
[2] A. Javey, J. Guo, Q. Wang, M. Lundstrom, H. Dai, Ballistic carbon nanotube field-effect transistors, Nature 424 (2003) 654–657.
[3] D. Zhang, K. Ryu, X. Liu, E. Polikarpov, J. Ly, M.E. Tompson, C. Zhou, Transparent, conductive, and flexible carbon nanotube films and their application in organic light-emitting diodes, Nano Letters 6 (2006) 1880–1886.
[4] J. Li, Y. Lu, Q. Ye, M. Cinke, J. Han, M. Meyyappan, Carbon nanotube sensors for gas and organic vapor detection, Nano Letters 3 (2003) 929–933.
[5] D. Lee, T. Cui, Low-cost, transparent, and flexible single-walled carbon nanotube nanocomposite based ion-sensitive field-effect transistors for pH/glucose sensing, Biosensors and Bioelectronics 25 (2010) 2259–2264.
[6] D. Lee, T. Cui, pH-dependent conductance behaviors of layer-by-layer self-assembled carboxylated carbon nanotube multilayer thin-film sensors, Journal of Vacuum Science and Technology B 27 (2009) 842–848.
[7] D. Lee, Y. Chander, S.M. Goyal, T. Cui, Carbon nanotube electric immunoassay for the detection of swine influenza virus H1N1, Biosensors and Bioelectronics 26 (2011) 3482–3487.
[8] A.B. Kaul, E.W. Wong, L. Epp, B.D. Hunt, Electromechanical carbon nanotube switches for high-frequency applications, Nano Letters 6 (2006) 942–947.
[9] S.W. Lee, D.S. Lee, R.E. Morjan, S.H. Jhang, M. Sveningsson, O.A. Nerushev, Y.W. Park, E.E.B. Campbell, A three-terminal carbon nanorelay, Nano Letters 4 (2004) 2027–2030.
[10] L.M. Jonsson, S. Axelsson, T. Nord, S. Vierfers, J.M. Kinaret, High frequency properties of a CNT-based nanorelay, Nanotechnology 15 (2004) 1497.
[11] D. Lee, T. Cui, Suspended carbon nanotube nanocomposite beams with a high mechanical strength via layer-by-layer nano-self-assembly, Nanotechnology 22 (2011) 165601.
[12] V. Pichot, S. Badaire, P.A. Albouy, C. Zakri, P. Poulin, P. Launois, Structural and mechanical properties of single-wall carbon nanotube fibers, Physical Review B 74 (2006) 245416.
[13] J.E. Fischer, W. Zhou, J. Vavro, M.C. Llaguno, C. Guthy, R. Haggenmueller, M.J. Casavant, D.E. Walters, R.E. Smalley, Magnetically aligned single wall carbon nanotube films: preferred orientation and anisotropic transport properties, Journal of Applied Physics 93 (2003) 2157–2163.
[14] F. Du, J.E. Fischer, K.I. Winey, Effect of nanotube alignment on percolation conductivity in carbon nanotube/polymer composites, Physical Review B 72 (2005) 121404.
[15] E. Camponeschi, R. Vance, M. Al-Haik, H. Garmestani, R. Tannenbaum, Properties of carbon nanotube–polymer composites aligned in a magnetic field, Carbon 45 (2007) 2037–2046.
[16] H. Ko, V.V. Tsukruk, Liquid-crystalline processing of highly oriented carbon nanotube arrays for thin-film transistors, Nano Letters 6 (2006) 1443–1448.
[17] M. Lu, M.-W. Jang, G. Haugstad, S.A. Campbell, T. Cui, Well-aligned and suspended single-walled carbon nanotube film: directed self-assembly, patterning, and characterization, Applied Physics Letter 94 (2009) 261903.
[18] S. Tawfick, M. De Volder, A.J. Hart, Structurally programmed capillary folding of carbon nanotube assemblies, Langmuir 27 (2011) 6389–6394.
[19] Y. Hayamizu, T. Yamada, K. Mizuno, R.C. Davis, D.N. Futaba, M. Yumura, K. Hata, Integrated three-dimensional microelectromechanical devices from processable carbon nanotube wafers, Nature Nanotechnology 3 (2008) 289–294.
[20] Z. Ye, D. Lee, S.A. Campbell, T. Cui, Thermally enhanced single-walled carbon nanotube microfluidic alignment, Microelectronic Engineering 88 (2011) 2919–2923.
[21] C.L. Pint, N. Nicholas, S.T. Pheasant, J.G. Duque, A.N.G. Parra-Vasquez, G. Eres, M. Pasquali, R.H. Hauge, Temperature and gas pressure effects in vertically aligned carbon nanotube growth from Fe–Mo catalyst, Journal of Physical Chemistry C 112 (2008) 14041–14051.
[22] Y. Zhang, G. Zou, S.K. Doorn, H. Htoon, L. Stan, M.E. Hawley, C.J. Sheehan, Y. Zhu, Q. Jia, Tailoring the morphology of carbon nanotube arrays: from spinnable forests to undulating foams, ACS Nano 3 (2009) 2157–2162.
[23] D. McIntosh, V.N. Khabashesku, E.V. Barrera, Benzoyl peroxide initiated in situ functionalization, processing, and mechanical properties of single-walled carbon nanotube-polypropylene composite fibers, Journal of Physical Chemistry C 111 (2007) 1592–1600.
[24] A. Heidelberg, L.T. Ngo, B. Wu, M.A. Phillips, S. Sharma, T.I. Kamins, J.E. Sader, J.J. Boland, A generalized description of the elastic properties of nanowires, Nano Letters 6 (2006) 1101–1106.

Biographies

Dongjin Lee received his B.S. and M.S. degrees from Korea University, Seoul, Korea in 2003 and 2005, respectively and obtained his Ph.D. degree from the University of Minnesota in 2010. He is currently Assistant Professor at the School of Mechanical Engineering, Konkuk University in Korea. He spent 19 months as Postdoctoral Research Associate at the University of Minnesota and Korea Advanced Institute of Science and Technology. From 2004 to 2005, he worked as a Guest Researcher at the

Nanoscale Metrology Group, National Institute of Standards and Technology (NIST), MD, USA. His main research topics include micro- and nanoelectromechanical systems (M/NEMS), nanomaterials, flexible electronics, energy and bio application of nanostructures, and general nanotechnology.

Zhijiang Ye received his M.S. degree from the University of Minnesota in 2010. His research interest is in M/NEMS, microfluidic and nanotechnology.

Stephen A. Campbell received his B.S. degree from College of St. Thomas in 1975, and obtained M.S. and Ph.D. degrees from Northwestern University in 1978. He is a Professor at the Department of Electrical and Computer Engineering, University of Minnesota. His area of expertise includes micro/nanofabrication, materials for deeply scaled devices, M/NEMS, semiconductor nanoparticles, nanoparticle devices, quantum dots, and QD-LEDs.

Tianhong Cui received his B.S. degree from Nanjing University of Aeronautics and Astronautics in 1991, and Ph.D. degree from the Chinese Academy of Sciences in 1995. He is currently a Professor of Mechanical Engineering at the University of Minnesota. From 1999 to 2003, he was an assistant professor of electrical engineering at Louisiana Technical University. Prior to that, he was a STA fellow at the National Laboratory of Metrology, and served as a postdoctoral research associate at the University of Minnesota and Tsinghua University. He received research awards including the Nelson Endowed Chair Professorship from the University of Minnesota, the Research Foundation Award from Louisiana Tech University, the Alexander von Humboldt Award in Germany, and the STA & NEDO fellowships in Japan. His current research interests include M/NEMS, nanotechnology, and polymer electronics.